Hindawi Publishing Corporation
ISRN Condensed Matter Physics
Volume 2013, Article ID 142029, 6 pages
http://dx.doi.org/10.1155/2013/142029

Research Article

Thickness-Dependent Physical Properties of Coevaporated Cu_4SnS_4 Films

V. P. Geetha Vani, M. Vasudeva Reddy, and K. T. Ramakrishna Reddy

Department of Physics, Sri Venkateswara University, Tirupati 517 502, India

Correspondence should be addressed to K. T. Ramakrishna Reddy; ktrkreddy@gmail.com

Received 17 May 2013; Accepted 17 June 2013

Academic Editors: S. Krukowski, Y. Ohta, T. Prokscha, and S. Wang

Cu_4SnS_4 films of different thicknesses were prepared by thermal coevaporation technique on glass substrates at a constant substrate temperature of 400°C. The layer thickness was varied in the range 0.25–1 μm. The composition analysis revealed that all the evaporated films were nearly stoichiometric. The XRD patterns indicated the presence of a strong (311) peak as the preferred orientation, following the orthorhombic crystal structure corresponding to Cu_4SnS_4 films. Raman analysis showed a sharp peak at 317 cm^{-1}, also related to Cu_4SnS_4 phase. The optical transmittance spectra suggested that the energy band gap decreased from 1.47 eV to 1.21 eV with increase of film thickness. The hot-probe test revealed that the layers had p-type electrical conductivity. A decrease of electrical resistivity was observed with the rise of film thickness.

1. Introduction

In recent years, extensive efforts have been made in finding novel and new semiconductors for application in energy conversion using the photovoltaic route. One such new material system is the Cu-Sn-S that contains inexpensive, nontoxic, and earth-abundant elements. This ternary system exhibited different stable phases such as Cu_2SnS_3, $Cu_2Sn_3S_7$, $Cu_5Sn_2S_7$, Cu_4SnS_4, and $Cu_{10}Sn_2S_{13}$, that was reported by Wu et al. [1]. All these compounds are represented by the general formula I-IV-VI. Their optimum optical, thermal, and mechanical properties with appropriate energy band gap of these materials have attracted much attention for their applications in solar cells, sensor and other optoelectronic devices [2]. Cu_4SnS_4 is one such material that had an optimum energy band gap for solar energy conversion along with suitable properties [3, 4]. Hence, many researchers have attempted to grow thin films of this material using a variety of wet chemical methods such as chemical bath deposition [5] and electrodeposition [6]. However, to our knowledge, there were no attempts made to form Cu_4SnS_4 films using physical methods. Therefore, thermal coevaporation technique has been used in this study for the growth of Cu_4SnS_4 films. It is one of the best techniques because of the possibility of large-scale production, high quality of the grown layers, and minimum wastage of components. In previous work, we have shown that thin films of Cu_4SnS_4 could be obtained by coevaporating SnS and CuS powders [7].

In general, the physical properties of thin films strongly depend on the deposition technique and growth parameters as well as the film thickness [8]. Film thickness plays an important role in controlling the film properties unlike its bulk counterpart, and all the physical properties of the films may oscillate with thickness [9–12]. The influence of crystallite size on the physical properties has been of much interest in semiconductor devices. The structure and surface morphology of the film changes with the increase of film thickness, which will in turn affect the optical transmittance [13, 14] and electronic properties [15, 16]. Hence, in the present work, the influence of film thickness on physical properties of Cu_4SnS_4 films has been investigated and reported.

2. Experimental Analysis

Cu_4SnS_4 thin films were prepared by thermal coevaporation technique using Box-type Hind Hi Vac system (model BC-300). 5N pure CuS and SnS were used as the source materials,

and the depositions were carried out under a pressure better than 10^{-5} Torr. In this technique, the distance between the source and substrate is maintained as 20 cm. The material is kept in a tantalum boat covered with quartz wool, which is heated by resistive heating process. Ultrasonically cleaned Corning 7059 glass slides were used as substrates for depositing Cu_4SnS_4 films. The films were prepared for different thicknesses that vary in the range 0.25–1 μm, keeping the substrate temperature at 400°C. The rate of deposition and thickness of the experimental films were determined using the quartz crystal thickness monitor (model QTM-101) placed just below the substrate holder. The as-grown layers were characterized by studying the composition, structural, optical, and electrical properties. The elemental composition and surface morphology of Cu_4SnS_4 films were examined using scanning electron microscope (SEM) (model: Zeiss EVO MA 15) attached to the energy dispersive X-ray analyser (EDAX) system (model: INCA Penta FET X3). The structural properties of Cu_4SnS_4 films were measured using an (model: Seifert 3003TT) X-ray diffractometer (XRD) with Cu-K_α radiation source (λ = 1.5402 Å). Raman analysis was carried out at room temperature with HORIBA JOBIN YVON (model: Lab Ram HR800) Raman spectrometer. The optical transmittance of the films was recorded as a function of wavelength using Perkin Elmer Lambda-950 UV-Vis-NIR spectrophotometer in order to determine the optical band gap, absorption coefficient, and refractive index. The electrical properties of the films were recorded by using hot-probe method, four-probe method, and Hall effect studies.

3. Results and Discussion

The as-grown Cu_4SnS_4 layers were pinhole free, uniform, and well adherent to the substrate surface. With the increase of film thickness, the color of the films was changed from pale-brownish yellow to dark-yellowish brown.

3.1. Compositional Analysis. The composition of the different elements present in Cu_4SnS_4 films, grown at a constant substrate temperature, was approximately constant although there is an increase of film thickness (t). Figure 1 shows the EDAX spectrum of a typical Cu_4SnS_4 film grown with a thickness of 1 μm. It can be seen from the spectrum that there were peaks corresponding to Cu, Sn, and S, and no other impurities were present. The elemental composition of the layer evaluated using this spectrum was Cu = 43.35 at. %, Sn = 15.56 at. %, and S = 41.09 at. %.

3.2. Structure and Phase Analysis. X-ray diffraction patterns of Cu_4SnS_4 thin films formed with different thicknesses are shown in Figure 2. The as-deposited Cu_4SnS_4 films were polycrystalline and exhibited different peaks that correspond to the (311), (121), (102), (112), (411), (022), (511), (222), (502), (512), (403), and (503) orientations of the Cu_4SnS_4. The films showed (311) plane as the dominant orientation, and its intensity increased with the increase of film thickness, which indicates an improvement in the crystallinity of the layers. The crystal structure was evaluated to be orthorhombic.

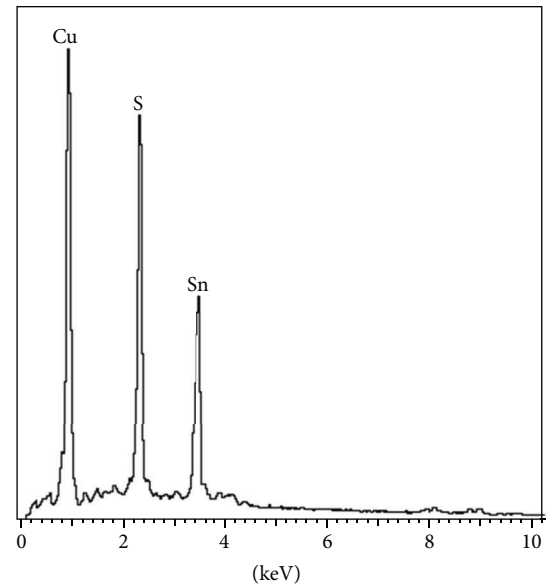

Figure 1: EDAX spectrum of Cu_4SnS_4 film with a thickness of 1 μm.

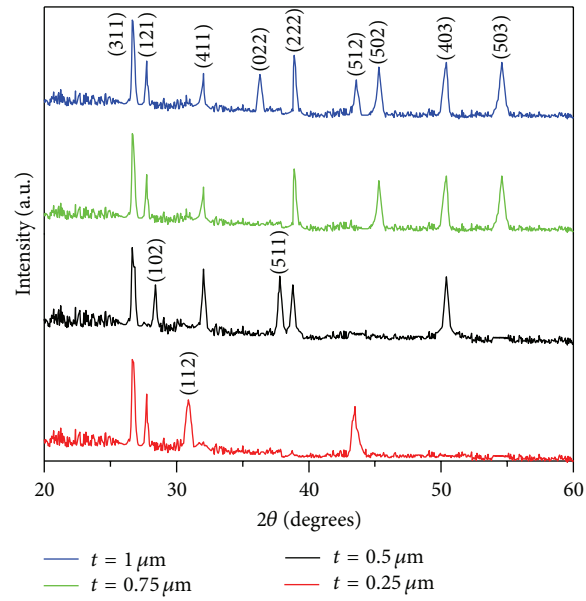

Figure 2: XRD spectra of Cu_4SnS_4 films prepared at a substrate temperature of 400°C.

Nair et al. [17] also observed a similar behavior with the (311) plane as preferred orientation in Cu_4SnS_4 films formed by heating SnS-CuS layers grown by chemical bath deposition method.

The lattice parameters corresponding to orthorhombic crystal structure were calculated using the relation

$$\frac{1}{d^2} = \frac{h^2}{a^2} + \frac{k^2}{b^2} + \frac{l^2}{c^2}, \quad (1)$$

where d is the interplanar distance and $(h\,k\,l)$ are the Miller indices. The evaluated lattice parameters were a = 13.52 Å, b = 7.67 Å, and c = 6.43 Å. The change in lattice parameters

a, b, and c with increase of film thickness was found to be marginal. The evaluated lattice parameters are in close agreement with the standard JCPDS data file (Card no. 29-0584). The crystallite size, D, of the as-deposited layers was evaluated using the Debye-Scherrer formula [18] given by

$$D = \frac{0.94\lambda}{\beta \cos\theta}, \quad (2)$$

where β is the full width at half maximum of the (311) peak, θ is the diffraction angle, and λ is the X-ray wavelength. The crystallite size of the films increased from 39 nm to 76 nm with the increase of film thickness. The increase in crystallite size might be interpreted in terms of columnar grain growth in the film structure. The observed less grain size at lower thicknesses might be due to the strong interaction between the substrate and vapour atoms, which restricts the mobility of ad-atoms. The improvement in the crystallinity of Cu_4SnS_4 layers can provide activation energy for the adsorbed atoms to occupy the minimum energy positions, enhancing the recrystallization due to the coalescence of the islands by increasing the volume and surface diffusions.

3.3. Raman Analysis. The Raman spectroscopy measurements were conducted on the as-grown Cu_4SnS_4 films in the wavenumber range 100–600 cm^{-1} as shown in Figure 3. From the Raman spectra, only one characteristic Raman line could be observed at 317 cm^{-1} for all thicknesses. This vibrational mode is not related to any other binary or ternary phases of Cu-Sn-S such as SnS, SnS_2, Sn_2S_3, CuS, Cu_2S, Cu_2SnS_3, and Cu_3SnS_4 and is therefore ascribed due to the contribution of Cu_4SnS_4 phase as it is also confirmed from the XRD analysis. It could be seen from the Raman spectra that the intensity of the peak increased with the increase of film thickness, which could be due to the improvement in the crystallinity of the layers.

3.4. Morphological Analysis. Figure 4 shows the SEM pictures of Cu_4SnS_4 films grown in the thickness range 0.25–1 μm. All the films showed worm-like grains that were uniformly distributed across the surface of the substrate. The size of the grains increased with the increase of the film thickness, and the layers became more densely packed with rough surface morphology. Cu_4SnS_4 films deposited at lower thicknesses <0.5 μm exhibited uniformly distributed small grains with regular shapes. Although the size of the grains is small, the grains were grown uniformly. The surface structure of the films grown at higher thicknesses >0.75 μm contained grains with complex and multiple structures. This is the evidence for the presence of Cu_4SnS_4 phases with different orientations in accordance with the XRD data. Here, the size of the grain is higher than in the films grown at other thicknesses.

3.5. Optical Properties. Figure 5 shows the optical transmittance of Cu_4SnS_4 films formed with different thicknesses where the transmittance of the films was recorded in the wavelength range 500–2500 nm. The spectra indicated a steep increase in the transmittance near the fundamental absorption, indicating the presence of direct optical transition

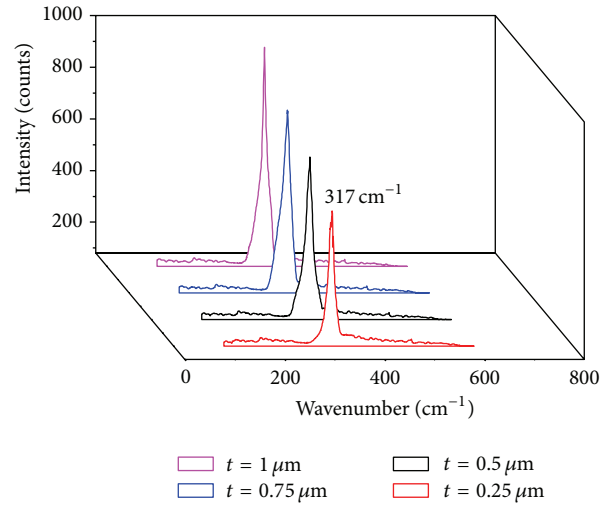

FIGURE 3: Raman spectra of Cu_4SnS_4 films deposited at different thicknesses.

in the films. With the increase of film thickness, the absorption edge was shifted towards longer wavelength side, indicating a decrease in the energy band gap of the films. In order to evaluate the energy band gap, E_g, of the films, $(\alpha h\nu)^p$ was plotted against the photon energy ($h\nu$), where p is an integer whose value reveals the type of optical transition in the films. In the present study, the nature of the transition was found to be direct, and the energy band gap was calculated using the relation [19]

$$(\alpha h\vartheta) = M\left(h\vartheta - E_g\right)^{1/2}, \quad (3)$$

where M is a constant, $h\nu$ is the incident photon energy, and α is the absorption coefficient, calculated using the relation

$$\alpha = \frac{-\ln(T)}{d}, \quad (4)$$

where T is the transmittance and d is the thickness of the film. The evaluated absorption coefficient of the layers was $>10^4$ cm^{-1}. Figure 6 shows the plots of $(\alpha h\nu)^2$ versus $h\nu$ where the extrapolation of the plot onto $h\nu$ axis gives the band gap. The energy band gap of the films decreased from 1.47 eV to 1.21 eV with the increase of film thickness from 0.25 μm to 1 μm. The energy band gap can be affected by the increase of crystallite size, decreasing of stacking faults and crystal imperfections, which results in the orientation of the individual crystallites [20], quantum size effect [21], and disorder at the grain boundaries [22]. In the present study, the change in energy band gap with film thickness can be understood by the decrease of structural disorder as well as increase in crystallite size in the films as observed from the microstructural analysis. Patel et al. also observed a similar behavior in CZTS films prepared by spray pyrolysis technique [23]. In our previous work [7], we observed that the energy band gap varied between 1.7 eV and 1.9 eV where the film thickness was approximately 200 nm, and the layers were grown using different substrate temperatures varied

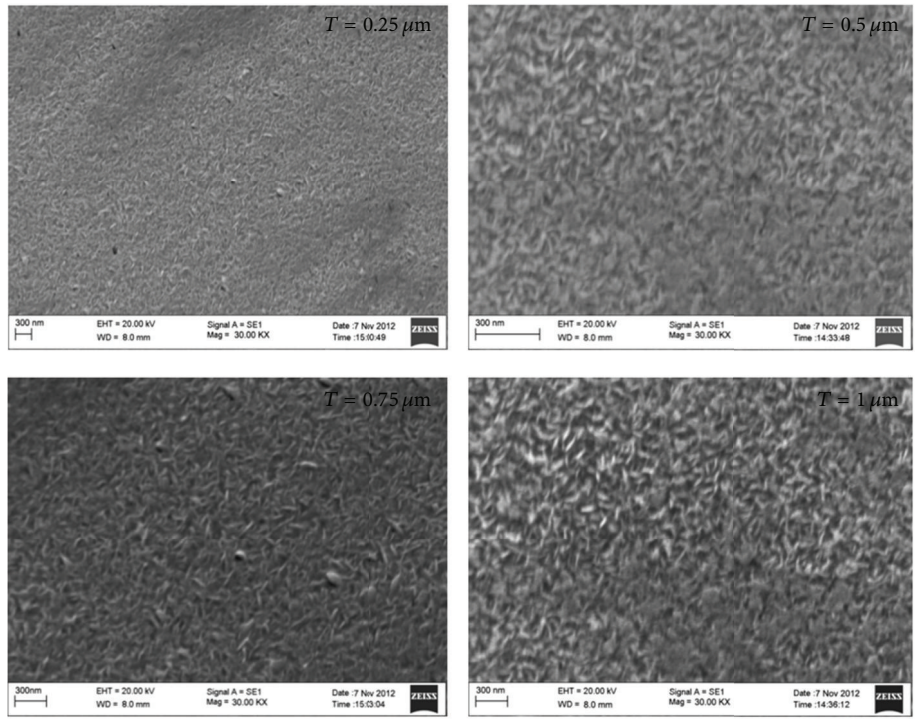

Figure 4: SEM pictures of as-deposited Cu_4SnS_4 films formed with different thicknesses.

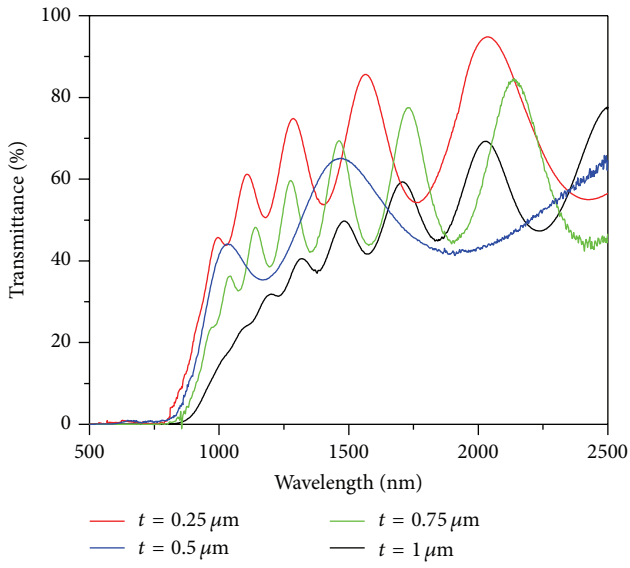

Figure 5: Transmittance versus wavelength spectra of Cu_4SnS_4 films.

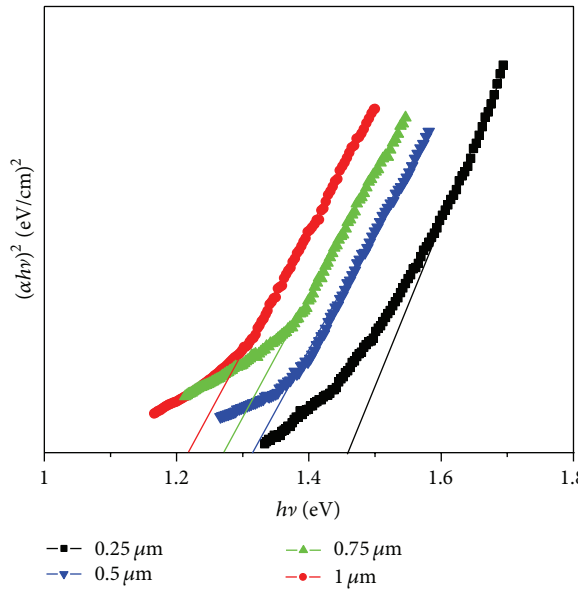

Figure 6: Plots of $(\alpha h\nu)^2$ versus $h\nu$.

in the range 200–350°C. These films showed that the crystallite size varied in the range 18–35 nm. Hence, the reported higher energy band gap in these layers is attributed to the quantum confinement due to small crystallite size. However, in this study, the layers thickness varied over a wide range of 0.25–1.0 μm, where the evaluated grain size varied from 39 nm to 76 nm. Therefore, the observed decrease in the band gap in the present work compared to our previous work is attributed to the improvement in the crystallite size.

3.6. Electrical Properties. The hot-probe test revealed that all the as-grown films exhibited p-type electrical conductivity. The electrical properties of the Cu_4SnS_4 layers were examined at room temperature by four-probe method and Hall effect studies. Figure 7 shows the variation of electrical resistivity with film thickness. The resistivity of the films decreased from $5.8 \times 10^2\ \Omega$ cm to $2.5 \times 10^2\ \Omega$ cm with the increase of film thickness from 0.25 μm to 1 μm. This decrease of film resistivity with thickness might be due to the decrease

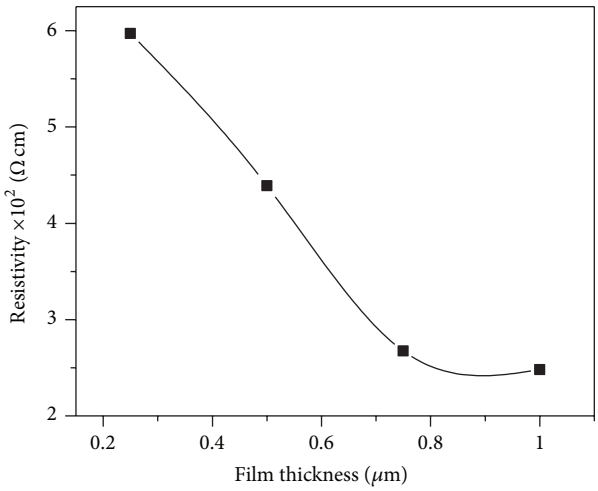

Figure 7: Variation of electrical resistivity with film thickness.

of residual stress and defect density with the increase of crystallite size in the films [24]. The increase of crystallite size could mainly decrease the grain boundary scattering thereby decreasing the film resistivity. The carrier concentration of the film increased from $9 \times 10^{14}\,\mathrm{cm}^{-3}$ to $3.6 \times 10^{15}\,\mathrm{cm}^{-3}$, and the mobility of the film decreased from $12\,\mathrm{cm}^2\,\mathrm{V}^{-1}\,\mathrm{s}^{-1}$ to $7\,\mathrm{cm}^2\,\mathrm{V}^{-1}\,\mathrm{s}^{-1}$. Avellaneda et al. [3] also reported similar observation for the thin films of Cu_4SnS_4 prepared by chemical bath deposition technique by heating SnS-CuS for 1 h each at different temperatures: 315, 350, and 400°C under 300 mTorr of nitrogen and the chamber was evacuated to about 20 mTorr.

4. Conclusions

Cu_4SnS_4 films have been successfully grown by thermal coevaporation of CuS and SnS on glass substrates at a substrate temperature of 400°C and varying the film thickness in the range 0.25–1 μm. The XRD patterns suggested that all the as-deposited films were polycrystalline in nature with the (311) plane as the preferred orientation and exhibited orthorhombic structure. The Raman studies revealed only a single peak corresponding to Cu_4SnS_4 phase. The films had high optical absorption, and the evaluated energy band gap decreased with the increase of film thickness and varied in the range 1.47–1.21 eV. The electrical resistivity of the films also showed a similar trend with the increase of film thickness.

Acknowledgments

V. P. Geetha Vani would like to thank the UGC, New Delhi, for financial assistance through the RFSMS-BSR fellowship.

References

[1] D. Wu, C. R. Knowles, and L. Y. Chang, "Copper-tin sulphides in the system Cu–Sn–S," *Mineralogical Magazine*, vol. 50, no. 2, pp. 323–325, 1986.

[2] G. Marcano, D. B. Bracho, C. Rincón, G. S. Pérez, and L. Nieves, "On the temperature dependence of the electrical and optical properties of Cu_2GeSe_3," *Journal of Applied Physics*, vol. 88, no. 2, pp. 822–828, 2000.

[3] D. Avellaneda, M. T. S. Nair, and P. K. Nair, "Cu_2SnS_3 and Cu_4SnS_4 thin films via chemical deposition for photovoltaic application," *Journal of the Electrochemical Society*, vol. 157, no. 6, pp. D346–D352, 2010.

[4] Q. Chen, X. Dou, Y. Ni, S. Cheng, and S. Zhuang, "Study and enhance the photovoltaic properties of narrow-bandgap Cu_2SnS_3 solar cell by p-n junction interface modification," *Journal of Colloid and Interface Science*, vol. 376, no. 1, pp. 327–330, 2012.

[5] A. Kassim, T. W. Tee, A. M. Sharif et al., "Influence of bath temperature and pH value on properties of chemically deposited Cu_4SnS_4 thin films," *Journal of the Chilean Chemical Society*, vol. 54, no. 4, pp. 345–348, 2009.

[6] K. Anuar, W. T. Tan, S. Atan et al., "Effects of electrolytes concentration on the chemically deposited Cu_4SnS_4 thin films," *Asian Journal of Chemistry*, vol. 22, no. 1, pp. 222–232, 2010.

[7] V. P. G. Vani, R. W. Miles, and K. T. R. Reddy, "Preparation and properties of Cu_4SnS_4 thin films," *Journal of Optoelectronic Engineering*, vol. 3, pp. 1–5, 2013.

[8] D.-A. Luh, T. Miller, J. J. Paggel, and T.-C. Chiang, "Large electron-phonon coupling at an interface," *Physical Review Letters*, vol. 88, no. 25 I, pp. 2568021–2568024, 2002.

[9] C. M. Wei and M. Y. Chou, "Theory of quantum size effects in thin Pb(111) films," *Physical Review B*, vol. 66, Article ID 233408, 4 pages, 2002.

[10] T. Valla, M. Kralj, A. Šiber et al., "Oscillatory electron-phonon coupling in ultra-thin silver films on V(100)," *Journal of Physics Condensed Matter*, vol. 12, no. 28, pp. L477–L482, 2000.

[11] O. Pfennigstorf, A. Petkova, H. L. Guenter, and M. Henzler, "Conduction mechanism in ultrathin metallic films," *Physical Review B*, vol. 65, no. 4, Article ID 045412, 8 pages, 2002.

[12] B. G. Orr, H. M. Jaeger, and A. M. Goldman, "Transition-temperature oscillations in thin superconducting films," *Physical Review Letters*, vol. 53, no. 21, pp. 2046–2049, 1984.

[13] F. Lai, M. Li, H. Wang et al., "Optical scattering characteristic of annealed niobium oxide films," *Thin Solid Films*, vol. 488, no. 1-2, pp. 314–320, 2005.

[14] R. Brüggemann, P. Reinig, and M. Hölling, "Thickness dependence of optical scattering and surface roughness in microcrystalline silicon," *Thin Solid Films*, vol. 427, no. 1-2, pp. 358–361, 2003.

[15] H. Kim, J. S. Horwitz, G. Kushto et al., "Effect of film thickness on the properties of indium tin oxide thin films," *Journal of Applied Physics*, vol. 88, no. 10, pp. 6021–6025, 2000.

[16] Z. Qiao, R. Latz, and D. Mergel, "Thickness dependence of In_2O_3 : Sn film growth," *Thin Solid Films*, vol. 466, no. 1-2, pp. 250–258, 2004.

[17] M. T. S. Nair, C. Lopéz-Mata, O. GomezDaza, and P. K. Nair, "Copper tin sulfide semiconductor thin films produced by heating SnS–CuS layers deposited from chemical bath," *Semiconductor Science and Technology*, vol. 18, no. 8, pp. 755–759, 2003.

[18] B. E. Warren, *X-Ray Diffraction*, Dover, New York, NY, USA, 1990.

[19] J. Tauc, *Amorphous and Liquid Semiconductors*, J. Tauc, Ed., chapter 4, Plenum, London, UK, 1974.

[20] C. D. Lokhande, A. U. Ubale, and P. S. Patil, "Thickness dependent properties of chemically deposited Bi_2S_3 thin films," *Thin Solid Films*, vol. 302, no. 1-2, pp. 1–4, 1997.

[21] S. Ilican, Y. Caglar, and M. Caglar, "Preparation and characterization of ZnO thin films deposited by sol-gel spin coating method," *Journal of Optoelectronics and Advanced Materials*, vol. 10, no. 10, pp. 2578–2583, 2008.

[22] N. Kumar, U. Parihar, R. Kumar, K. J. Patel, C. J. Panchal, and N. Padha, "Effect of film thickness on optical properties of tin selenide thin films prepared by thermal evaporation for photovoltaic applications," *American Journal of Materials Science*, vol. 2, pp. 41–45, 2012.

[23] M. Patel, I. Mukhopadhyay, and A. Ray, "Structural, optical and electrical properties of spray-deposited CZTS thin films under a non-equilibrium growth condition," *Journal of Physics D*, vol. 45, Article ID 445103, 10 pages, 2012.

[24] K. L. Chopra, *Thin Film Phenomena*, McGraw-Hill, New York, NY, USA, 1969.